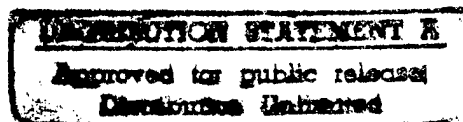


Hanson PD, Warner C, Kofroth R, Osmond C, Bogdanske JJ, Kalscheur VL, Frassica FJ, Markel MD. The Effect of Intramedullary Polymethylmethacrylate and Autogenous Cancellous Bone on Healing of Frozen Segmental Allografts. Abstract submitted to the International Society of Limb Salvage meeting, to be held September, 1997.

19970506 071



DTIC QUALITY INSPECTED 3

# THE EFFECT OF INTRAMEDULLARY POLYMETHYLMETHACRYLATE AND AUTOGENOUS CANCELLOUS BONE ON HEALING OF FROZEN SEGMENTAL ALLOGRAFTS

Hanson PD, Warner C, Kofroth R, Osmond C, Bogdanske JJ, Kalscheur VL, Frassica FJ, and Merkel MD. Comparative Orthopaedic Research Laboratory, School of Veterinary Medicine, University of Wisconsin, 2015 Linden Dr. West, Madison, WI 53706

**Background.** Bone allografts remain a good method of repair for segmental defects. Even so, fracture, delayed union and non-union remain significant complications. Until growth factor modulation and synthetic techniques become standard clinical practice, other methods of improving allograft incorporation are required.

**Objective/Hypothesis.** This study was designed to compare the effects of intramedullary bone cement and autogenous cancellous bone on limb function, remodeling activity, and incorporation of mid-diaphyseal segmental allografts of the femur stabilized with an interlocking nail (ILN) technique in a dog model.

**Methods.** Twenty-four mature beagle dogs, weighing 10-15 kg each, were randomly divided for bilateral frozen allograft replacement of the mid-diaphysis (2.5-cm) of the femur. All allografts were from immunologically mismatched donors. Allograft stabilization was performed with an ILN technique. Treatments were randomly assigned to left and right legs as follows: group 'n' = ILN alone (n=11), 'nc' = ILN plus intramedullary cement (n=11), 'ncp' = ILN plus intramedullary cement and autogenous cancellous bone placed periosteally (n=6), 'np' = ILN plus cancellous bone placed periosteally (n=7), 'ne' = ILN plus cancellous bone placed within the allograft (n=7), and 'npe' = ILN plus cancellous bone placed periosteally and within the allograft (n=6). Peak vertical ground reaction force, callus area, and BMD were determined at intervals from surgery to 24 weeks after surgery. Continuous labeling of new bone was achieved with daily oral tetracycline treatment. All animals were euthanized 24 weeks after surgery. Bone was processed to 100  $\mu$ m thick sections to determine microradiographic porosity, fluorescent new bone, and histologic grading. The mean ( $\pm$  SEM) of each parameter was determined. Statistical analysis was performed using ANOVA, with significance defined as  $P < 0.05$ .

**Results.** There were no differences between treatments for limb function or BMD. Callus area for treatments receiving periosteal cancellous bone was greater along the lateral and cranial surfaces 4 weeks after surgery and along the caudal surface at 24 weeks. New bone within the allograft segment did not differ between treatments. New bone at the host-allograft junctions was increased in treatments 'np' and 'npe'. Histologic scores were greatest with treatments 'ncp' and 'npe'. Bone union for treatment 'nc' was less than that for treatments 'ncp', 'np', and 'npe'. At the distal osteotomy, the remaining gap with treatment 'nc' was greater than other treatments.

**Conclusions.** The biologic properties suggest that ILN augmentation with intramedullary cement by itself is not recommended. However, there appear to be advantages to augmenting ILN fixation with a combination of (1) autogenous cancellous bone applied to the endosteal surface of the allograft and the periosteal surface of the host-allograft junctions or (2) autogenous cancellous bone applied to the periosteal surface of the host-allograft junctions and intramedullary PMMA cement around the ILN.

**Keywords.** allograft, fracture, limb salvage

***The Effect of Intramedullary Polymethylmethacrylate and Autogenous  
Cancellous Bone on Healing of Frozen Segmental Allografts***

Peter D. Hanson, Chad Warner, Rachael Kofroth, Christian Osmond, John J. Bogdanske,  
Vicki L. Kalscheur, Frank J. Frassica\*, and Mark D. Markel

From the Comparative Orthopaedic Research Laboratory, School of Veterinary Medicine,  
University of Wisconsin, and \*Department of Orthopaedic Surgery,

Johns Hopkins Medicine.

February, 1997

### Abstract

This study was designed to compare limb function, bone mineral density, periosteal callus, new bone, porosity, histology, and union of mid-diaphyseal segmental allografts of the femur stabilized with an interlocking nail (ILN) technique in a dog model. An *in vivo* study was performed to compare the effects of augmenting ILN fixation with the following : ILN alone (n), ILN plus intramedullary cement (nc), ILN plus intramedullary cement and autogenous cancellous bone applied to the periosteal surface of the host-allograft junction (ncp), ILN plus autogenous cancellous bone applied to the endosteal surface of the allograft (ne), ILN plus autogenous cancellous bone applied to the periosteal surface of the host-allograft junction (np), and ILN plus autogenous cancellous bone applied to the periosteal surface of the host-allograft junction and to the endosteal surface of the allograft (npe). Following allograft implantation, the dogs were evaluated by radiography, dual energy X-ray absorptiometry, and force plate gait analysis from 0 to 24 weeks. Six months after allograft implantation, the dogs were euthanatized and the femora processed for analysis. There were no differences between treatments for limb function or bone mineral density. Callus area 4 weeks after surgery was greater along the lateral and cranial surfaces for treatments receiving periosteal cancellous bone ( $P<0.05$ ). This was also evident along the caudal surface at 24 weeks ( $P<0.05$ ). New bone within the allograft segment did not differ between treatments and was reduced compared to the host-allograft junctions ( $P<0.05$ ). Histologic scores were greatest with treatments 'ncp' and 'npe', listed above ( $P<0.05$ ).

Union scores for treatment 'nc' were less than those for treatments 'ncp', 'np', and 'npe' ( $P<0.05$ ). At the distal osteotomy, the remaining gap with treatment 'nc' was greater than other treatments ( $P<0.05$ ).

## Introduction

Bone allografts remain one of the best methods for repair of segmental defects. Use of fresh allografts, either free or vascularized, is associated with large host immune responses unless immunosuppressive drugs are also administered.<sup>1-3</sup> Deep freezing of allografts greatly reduces the host immune response and eliminates the need for immunosuppressive drugs.<sup>1</sup> The advantages of frozen bone allografts for the treatment of segmental defects lies in the ability to store large numbers of these specimens for future use, allow selection of the proper shape, maintain normal bone structure, preserve some osteoinductive potential, and have greater strength than other techniques.<sup>4</sup>

Fracture of frozen segmental allografts remains a serious complication, with long term studies indicating occurrences of 10 to 19 percent.<sup>5-8</sup> Fracture risk is reportedly low during the first 6 months after surgery, but then increases over the next 2 years.<sup>5</sup> This time period corresponds to the remodeling phase of the allograft. Approaches to reduce the occurrence of fractures include avoiding placement of hardware through the allograft itself and augmenting fixation with methylmethacrylate.<sup>9-13</sup> In a large series of cases, Harrington found no evidence that the presence of methylmethacrylate in the medullary canal interferes with union.<sup>11</sup> However, when polymethylmethacrylate was used to lute dynamic compression plates in a dog model, Roush found decreased vascularity and increased porosity in the outer one third of the cortex at 5 weeks.<sup>14</sup> Straw *et al.* demonstrated that medullary cementation did not deter allograft-host bone union.<sup>12</sup>

However, histologic features were altered. These changes included an increased percent eroded surface, decreased percent osteoblast surface, and less fluorescence of new bone at endosteal regions.

Other complications of transplantation with allogeneic bone include delayed union and non-union of one or both host-allograft bone junctions. This complication may result as a consequence of the host immune response, a delay in revascularization, inadequate osteoprogenitor numbers, or a combination of these factors. The concurrent use of autogenous bone graft has been demonstrated to enhance allograft bone incorporation under various conditions by accelerating the healing process. Some authors suggest that autogenous cancellous autograft at the host-allograft junction is important for clinical success.<sup>15-20</sup> Owing to problems with donor site morbidity, some surgeons do not apply autogenous bone graft at the original surgery, but rather only apply bone graft to the junction if radiographic evidence of delayed union ensues. Studies with porous coated implants and freeze-dried allogeneic cancellous bone have demonstrated that cancellous allograft also aids repair, but that only autograft enhances new bone formation.<sup>19</sup> Long term follow up of human patients with segmental allograft bone have indicated that much of the graft remains unremodeled and that most of the remodeling activity occurs at the host-allograft junction and periosteal surface.<sup>21</sup> Identifying means to enhance overall graft incorporation would be desirable. Such enhancement may come from variations in application of cancellous autograft or through addition of appropriate growth factors.

This study was designed to investigate the effects of intramedullary polymethylmethacrylate and three autogenous bone graft methods on host-allograft bone union, limb function, and allograft remodeling. An *in vivo* dog model using an interlocking nail technique and 2.5-cm intercalary segment was used to examine these issues. It was hypothesized that intramedullary cement would increase the structural properties of the constructs, leading to improved physical and biologic properties at the study end point. It was hypothesized that the addition of autogenous cancellous bone would accelerate healing processes, leading to greater incorporation of the allograft by the study end point.

## Methods

*Surgical Technique* – Under an institutional review board approved protocol, 25 mature beagle dogs (one initial donor and 24 treatment animals), weighing 10-15 kg each, were used for bilateral frozen allograft replacement of the mid-diaphysis (2.5-cm) of the femur. All dogs were evaluated pre-operatively by standard radiography, dual energy X-ray absorptiometry (DXA), and force plate gait analysis. Dogs received prophylactic antibiotic therapy (cefazolin) and pain medication (butorphanol) at the induction of anesthesia and 4 hours later. Antibiotic therapy was continued for 14 days after surgery using oral enrofloxacin and metronidazole. Anesthesia was induced with an injectable technique (thiopental) and maintained with halothane in oxygen. In all cases, allografts were from immunologically mismatched donors. Mismatching was documented using dogs with a mixed lymphocyte reaction stimulation index of ten or greater.<sup>22</sup> Allograft stabilization was performed with an interlocking nail (ILN) technique (Figure 1). A lateral approach to the femur was performed and step-cut osteotomies were made in the proximal and distal diaphyses 2.5-cm apart. The step overlap with host bone was 0.5-cm in length. Harvested bone had the marrow and periosteum removed. The bone was quick frozen in liquid nitrogen and thawed in sterile saline at room temperature for two repetitions. It was then wrapped in saline soaked gauze and stored in sterile sealed bags at -80°C until subsequent use. The allograft bone harvested from the previous dog was thawed in warm sterile saline prior to use. Nail diameter (5 or 6-mm) and length (9.0 to 10.8-cm) were chosen to fit the

medullary canal based on pre-operative radiographs of each dog. Reaming of the medullary canal was performed as necessary. For bones receiving autogenous cancellous bone, the cancellous graft was harvested from the proximal and distal aspects of the femur at sites distant to the diaphyseal segment. These areas would have been disrupted by the ILN during nail placement. The quantity of cancellous bone harvested was recorded for each animal. The cancellous bone was then wrapped in a blood soaked sponge until used. Cancellous bone was packed in the medullary canal of the allograft prior to nail insertion, along the periosteal surface at each osteotomy prior to closure, or a combination of both techniques. For bones receiving PMMA cement, the PMMA was injected under pressure to fill the medullary canal of the allograft prior to nail insertion. The ILN was inserted in normograde fashion from the trochanteric fossa. A stainless steel dam with a hole the diameter of the ILN was used at the distal osteotomy during nail insertion to retain PMMA (if present) within the allograft. Care was taken to remove cement that entered any gap at the host-allograft junctions. Each osteotomy was further stabilized with a single cerclage wire (0.8-mm diameter) secured with a standard twist-knot. Two 2.7-mm screws were placed through the host bone and nail proximal to the allograft and two screws were placed distal to the allograft to complete the fixation.

*Treatment Allocation and Randomization* – Dogs were ordered for surgery based on immunologic mismatching and then randomly allocated into four groups with treatments randomly assigned to left and right legs as follows: *Group 1 (5 dogs)* – in one limb the

allograft was stabilized with an ILN (treatment 'n') and in the contralateral limb the allograft medullary canal was first filled with PMMA and then stabilized with an ILN (treatment 'nc'); *Group 2 (6 dogs)* – in one limb treatment 'n' was performed and in the contralateral limb autogenous cancellous bone was packed within the allograft medullary canal, stabilized with an ILN, and then autogenous cancellous bone packed along the periosteal surface at the host-allograft junctions (treatment 'npe'); *Group 3 (7 dogs)* – in one limb autogenous cancellous bone was packed within the allograft medullary canal, followed by stabilization with an ILN (treatment 'ne'), and in the contralateral limb autogenous cancellous bone was applied periosteally at the host-allograft junctions, followed by stabilization with an ILN (treatment 'np'); *Group 4 (6 dogs)* – in one limb treatment 'nc' was performed and in the contralateral limb the allograft medullary canal was first filled with PMMA, stabilized with an ILN, and then autogenous cancellous bone packed along the periosteal surface at the host-allograft junctions (treatment 'ncp')(Table 1). The overall distribution of treatments resulted in the following: treatment 'n' – 11 bones, treatment 'nc' – 11 bones, treatment 'ncp' – 6 bones, treatment 'np' – 7 bones, treatment 'ne' – 7 bones, and treatment 'npe' – 6 bones.

*Post-Operative Follow-up* – Radiography (mediolateral and craniocaudal views) was performed immediately after surgery and subsequently at 2, 4, 12, and 24 weeks later. Radiographic images were digitized and evaluated for callus area (NIH Image v1.59, National Institutes of Health, Bethesda, MD). Measurement calibration was performed with

each radiograph using the known diameter of the ILN as the reference. The total callus area present along the medial, lateral, cranial, and caudal surfaces of the bones was determined at 4, 12, and 24 weeks (Figure 2). Additionally, the total allograft area (allograft plus callus along the allograft) was determined at these time points and compared to the allograft area immediately after surgery.

Force plate gait analysis was performed pre-operatively and subsequently at 4, 12, and 24 weeks after surgery using a force plate (OR6-6-1000 Biomechanics Platform with SGA6-4 Signal Conditioner/Amplifier, Advanced Medical Technology Inc., Newton, MA) connected to a commercially available satellite data acquisition system (VETDATA v2.03, Acquire v5.0, Mininet v4.0 and Update v1.1 from Sharon Software Inc, Dewitt, MI), as previously described.<sup>23,24</sup> A single handler trotted dogs over the force plate at constant velocity. An observer monitored each trial to confirm foot strikes and gait. A trial was considered successful if a fore paw contacted the force plate and was then followed by contact of the ipsilateral hind paw. Three successful passes for each treatment limb were recorded at each time point. Output peak vertical force values were normalized to body weight and pre-operative values for comparison between treatments and across time within a treatment.

DXA scans were performed in a craniocaudal direction of each femur pre-operatively, immediately after surgery, and subsequently at 12 and 24 weeks later (QDR-1000/W, Hologic Inc., Waltham, MA). Pre-operative, 12, and 24 week scans were

performed with the dog sedated (acepromazine and butorphanol). The scan immediately after surgery was performed while the dog was still anesthetized. The dual energy X-ray source (70/140 kVp) had a resolution of 3.0-mm. The "prosthetic hip" algorithm was used to evaluate bone mineral density (BMD) from 8 regions of interest from each femur (Figure 3). The implant device (ILN and screws) was automatically removed from analysis, using a segmentation algorithm based on the metal's X-ray attenuation. Since the presence of ILN fixation has been shown to affect the measured BMD, paired comparisons were performed between the post-operative scan and scans 12 and 24 weeks later.<sup>25</sup>

All dogs received oral tetracycline (500 mg) daily beginning 2 weeks after surgery to label new bone formation. In all groups, dogs were euthanized with an overdose of barbiturate 24 weeks after surgery. The bones were harvested immediately, the ILN carefully removed to prevent disruption of callus, and the constructs potted for mechanical testing. The bones were then mechanically tested and the data analyzed as described in a companion paper.<sup>26</sup> Following mechanical testing, the bones were removed from the potting material and placed in containers with 70% ethanol for storage until histologic processing. Bones were processed for undecalcified histologic analysis as has been previously described.<sup>27,28</sup> Briefly, tissue was dehydrated in increasing concentrations of ethanol, followed by acetone. Infiltration and embedding were performed with methylmethacrylate under vacuum. The resulting blocks were trimmed with a band saw. The bone, including the allograft with adjacent proximal and distal host bone, was sectioned

on the mid-sagittal plane using a low-speed diamond saw set at 350 rpm and 600 g load (ISOMET PLUS Precision Saw, Buehler, Lake Bluff, IL). Three 200- $\mu\text{m}$  thick sagittal sections were cut, and the remaining bone halves were glued back together with cyanoacrylate. After repositioning the bone, three 200- $\mu\text{m}$  thick transverse sections were cut at each of 5 locations along the bone: proximal host bone, proximal host-allograft junction, allograft, distal host-allograft junction, and distal host bone (Figure 4). Implant hardware (cerclage wire) and radiographs were used to locate landmarks for consistent site selection. All sections were stored in a light-impervious box to protect fluorochrome labeling when not being processed or evaluated. Each section was subsequently ground to 100- $\mu\text{m}$  thick on a speed lapping machine (ML-521D, Maruto Instrument Co., Tokyo) set at 80 rpm and a pressure of 0.7 kg/cm<sup>2</sup>.

Fine detail contact microradiography, using a vacuum technique, was performed on one section from each location (14 kVp, 2 min.; Model 43855A, Hewlett-Packard Faxitron, McMinnville, OR). Once microradiography was completed, these unstained sections were mounted on microscope slides for fluorochrome label analysis. The resulting radiographs were examined on a microscope and digitized for semi-automated image analysis by a commercially available software package (MicroComp, Southern Micro, Atlanta, GA). Regions of interest were selected from new bone at the periosteal surface, mid-cortical bone, and new bone at the endosteal surface from 4 quadrants at each section location

(Figure 4). Owing to transverse sections having a glue seam at the cranial and caudal surfaces, regions of interest from these quadrants were selected from the corresponding location on the sagittal sections. Medial and lateral quadrant regions were selected from the transverse sections. The threshold level was manually adjusted to distinguish bone and pore space. The percent porosity was recorded for each region of interest. Evidence of bony union at quadrants from each host-allograft junction was scored a 1 if present and a 0 if absent. Partial union was defined as evidence of union at one or more quadrants from a given junction. Complete union was defined as evidence of union at all 4 quadrants from a given junction.

New bone formation was measured on a commercially available image analysis system (OsteoMeasure, OsteoMetrics Inc., Atlanta, GA). Unstained slides were examined under ultraviolet light. Regions of interest were chosen to correspond with those evaluated for porosity (Figure 4). Fluorescent new bone area was manually traced. The percent fluorescence of the field was converted to the percentage of total area of bone surface using the porosity data previously obtained for the same region of interest in the same section.

The remaining 2 sections from each location were stained for histologic analysis. One section was stained with a modified toluidine blue method for undecalcified sections, which included a 3 min surface etching with 0.2% formic acid.<sup>28</sup> The other section was stained with a modified Goldner's trichrome method for undecalcified sections, which included a 40 min immersion in 40% ethanol and a 1 min surface etching with 0.2% formic

acid.<sup>28</sup> The relative amounts of bone, cartilage, and fibrous tissue were scored at 4 quadrants of the proximal and distal host-allograft junctions (Figure 5). A modified scoring system was used to give each tissue type a score from 0 to 4, corresponding to the amount of that tissue present (0: none, 1: 1-25%, 2: 26-50%, 3: 51-75%, and 4: 76-100%).<sup>29</sup> The presence of bony union at each quadrant was scored, receiving a 1 if present and a 0 if absent. Partial and complete union were defined similar to that for evaluation from microradiographs. Any gap present, defined as non-bone tissue between host bone and allograft, was measured using a stage micrometer. An attempt was made to determine whether the gap was an artifact created by previous mechanical testing of the specimen.

The mean and SEM were determined for each property of interest. Statistical analysis was performed using the general linear models technique for ANOVA (The SAS System for Windows, Release 6.11, SAS Institute Inc., Cary, NC). When significance was present, means were separated by Duncan's multiple range test. Where appropriate, means were adjusted for other terms in the model using the least-squares means statement. Paired comparisons, contrasting differences between time points for an individual animal or analysis techniques, were evaluated by paired *t*-tests. Time series data (bone mineral density and gait analysis) were evaluated by repeated measures analysis of variance. Significance for all analyses was set at  $P < 0.05$ .

## Results

For treatments including autogenous cancellous bone, there was no difference in the quantity of cancellous bone harvested and applied ( $P>0.05$ )(Table 2). The overall mean quantity of cancellous autograft was  $0.5 \pm .02$  g. All dogs were ambulatory within two days after surgery. One dog from Group 4 became lame 6 weeks prior to sacrifice. At necropsy of this dog, one femur had evidence of chronic, low grade infection. Even though the contralateral limb had achieved complete union, data from this dog was not included in the analysis.

*Callus Area* – Radiographic evaluation of callus formation along the lateral, medial, cranial, and caudal surfaces of the bones revealed few significant differences between treatment groups at the times assessed. Four weeks after surgery there was greater callus area along the lateral surface of treatment 'np' than all other treatments except 'ncp' ( $P<0.05$ )(Table 3). Along the cranial surface, treatment 'npe' had greater callus area than treatment 'nc'( $P<0.05$ ). There was no significant difference between treatments at each surface 12 weeks after surgery ( $P>0.05$ ). At 24 weeks after surgery, treatments 'ncp' and 'np' had greater callus area than treatments 'n', 'nc', and 'ne' along the caudal surface ( $P<0.05$ ). When data from the 4 surfaces was pooled for each treatment, at 4 weeks after surgery the 3 treatments with autogenous cancellous bone added to the periosteal surface ('np', 'ncp, and 'npe') had greater callus area than the 3 treatments without added cancellous bone ('n', 'nc', and 'ne')( $P<0.05$ ). By 24 weeks after surgery, the only

difference in combined area was that treatment 'np' had greater area than treatment 'nc' ( $P<0.05$ ).

The mean size of all allografts was increased at 4, 12, and 24 weeks after surgery compared to immediately post-operatively. The increase in size came from callus along the allograft surface. However, this change in size was not significantly different between treatments at each time point ( $P>0.05$ )(Table 3). It was generally apparent that allograft size increased from 0 to 12 weeks after surgery and then reduced from 12 to 24 weeks. The only exceptions to this were present in the mediolateral radiographic views of treatments 'ncp' and 'np', which continued to increase in size with time.

*Bone Mineral Density* – Evaluation of bone mineral density of the entire femur and 7 regions-of-interest by DXA demonstrated no differences between treatments at any time point ( $P>0.05$ )(Table 4). Despite subtracting the ILN from analysis, BMD was increased immediately post-surgery compared to pre-operative evaluation for almost all treatments in the following regions: entire femur (Global), length of femur equivalent to length of ILN (R1), proximal host bone (R2), and distal host bone (R6)( $P<0.05$ ). Comparing the BMD immediately post-surgery with that at 12 and 24 weeks, the femoral head region (R7) from all treatments lost BMD during the initial 12 weeks and then remained at a steady-state ( $P<0.05$ ). Similarly, BMD of the entire femur (Global) decreased in 4 treatments ('n', 'nc', 'ne', and 'npe') by 12 weeks and then remained at a steady-state ( $P<0.05$ ). In the allograft

region (R4), only treatment 'n' had a decrease in BMD over time compared to its immediate post-surgery value ( $P<0.05$ ).

*Gait Analysis* – Peak vertical ground reaction forces expressed as the percent of pre-operative values were not significantly different between treatments at 4, 12, or 24 weeks for treated rear limbs or untreated fore limbs ( $P>0.05$ )(Figure 6). Evaluated by repeated measures analysis of variance, there was a significant overall time effect for treated rear limbs. Pooling data from all treatments, the peak vertical ground reaction force at 4 weeks was less than that pre-operatively or at 12 weeks ( $P<0.05$ )(Figure 7).

*Osteotomy Union* – Bone union at each osteotomy was graded separately from microradiographs and stained sections. Within a treatment, the only difference between the two evaluation techniques was the partial union score for treatment 'n' at the proximal host-allograft junction. In this case, microradiography indicated a higher score than histology ( $P<0.05$ ). Combining treatment data to evaluate patterns of union relative to bone quadrants, it was evident that union was greater at the lateral and medial quadrants than the cranial and caudal quadrants ( $P<0.05$ ). Comparing treatments, there was no difference in partial union for the proximal or distal host-allograft junctions. However, when applying the more strict requirement of complete union, at the proximal host-allograft junction treatment 'npe' had greater union than treatment 'nc' ( $P<0.05$ )(Figure 8). Similarly, at the distal host-allograft junction treatment 'np' had greater complete union than treatments 'ne' and 'nc', and treatment 'ncp' also had greater complete union

than treatment 'nc' ( $P < 0.05$ ). Comparing differences in union between the proximal and distal host-allograft junctions, overall there was greater partial union at the distal site (85.7% compared to 69.4%;  $P < 0.05$ ). There was no osteotomy difference for complete union.

*Porosity* – Bone porosity measured from microradiographs revealed a difference between quadrants (lateral, medial, cranial, and caudal) for a given treatment in 4 of 90 possible section (proximal host, proximal host-allograft junction, allograft, distal host-allograft junction, and distal host) and region (new periosteal bone, mid-cortical bone, and new endosteal bone) comparisons ( $P < 0.05$ ). Within a given quadrant, there were differences between treatments in 2 of 60 possible comparisons ( $P < 0.05$ ). Therefore, region porosity was evaluated using the mean of all quadrants for a given treatment and section. Overall, considering all treatments together, endosteal regions had greater porosity than periosteal regions, which had greater porosity than mid-cortical regions ( $P < 0.05$ ). Within the endosteal region, the distal host bone had greater porosity than the allograft, proximal host-allograft junction, and distal host-allograft junction ( $P < 0.05$ )(Figure 9).

Treatment differences were evaluated for a given region and section (Table 5). Bone porosity in the periosteal region had significant differences among treatments at 3 sections ( $P < 0.05$ ). At the proximal host-allograft junction, treatment 'npe' had greater porosity than treatment 'n'. Within the allograft, treatment 'npe' had greater porosity

than all other treatments except 'np'. At the distal host-allograft junction, treatment 'npe' had greater porosity than treatments 'ne' and 'nc'. Porosity of the mid-cortical region had differences among treatments at 2 sections ( $P<0.05$ ). Within the allograft, treatments 'npe' and 'ncp' had greater porosity than treatment 'np'. In the distal host bone, treatment 'npe' had greater porosity than treatment 'ne'. Porosity of the endosteal region had differences among treatments at 2 sections ( $P<0.05$ ). In the proximal host bone, treatments 'npe' and 'n' had greater porosity than treatments 'np', 'nc', and 'ne'. At the distal host-allograft junction, treatment 'np' had greater porosity than treatment 'ne'.

*Histologic Scoring* – Tissue at the host-allograft junction ranged from being indistinguishable from host bone to having a definite gap between host and allograft bone. Evaluation of tissue present at the osteotomies indicated overall differences between the proximal and distal host-allograft junctions. Distally there was more bone than proximally, and proximally there was more fibrous tissue than distally ( $P<0.05$ )(Table 6). The overall mean gap was also greater proximally than distally ( $P<0.05$ ). Comparing bone quadrants, there was greater overall amounts of bone at lateral and medial quadrants than cranial and caudal quadrants ( $P<0.05$ )(Table 7). Conversely, the amount of cartilage present was greater at cranial and caudal quadrants than lateral and medial quadrants.

Differences between treatments were present for all tissue types at each osteotomy. At the proximal host-allograft junction, treatment 'npe' had greater bone and

less fibrous tissue than all other treatments ( $P<0.05$ )(Figure 10). Treatments 'n' and 'nc' had more cartilage than treatment 'ne'. There was greater overlap of scores at the distal host-allograft junction. Treatment 'nc' had less bone and more fibrous tissue than all treatments except 'ne' ( $P<0.05$ ). Treatments 'ne' and 'npe' had more cartilage than treatment 'ncp'.

Many osteotomies had at least one cortex in which a gap remained between host and allograft bone. Often this gap was filled with fibrous or cartilaginous tissue that stained to suggest it was mineralizing. In other cases, periosteal callus was bridging from host bone to the allograft, but had not yet reached the allograft surface. There were differences in the mean gap distance for treatments at each osteotomy. At the proximal host-allograft junction, treatment 'nc' had a greater mean gap than treatment 'npe' ( $P<0.05$ )(Figure 11). Similarly, at the distal host-allograft junction, treatment 'nc' had a greater mean gap than all other treatments. There was no evidence of cement present in gaps from PMMA treated animals. It either was absent in the areas observed, fell out during tissue processing, or was not a factor in gap formation.

*New Bone* – Tetracycline labeled new bone measurements revealed a difference between quadrants (lateral, medial, cranial, and caudal) for a given treatment in 2 of 54 possible section and region comparisons ( $P<0.05$ ). Within a given quadrant, there were differences between treatments in 3 of 36 possible comparisons ( $P<0.05$ ). Therefore, as with porosity measurements, region new bone was evaluated using the mean of all

quadrants for a given treatment and section. Considering all treatments together, endosteal and periosteal regions had more new bone at the proximal and distal host-allograft junctions than mid-cortical regions ( $P<0.05$ ). In the allograft, periosteal new bone was greater than endosteal new bone, which was greater than mid-cortical new bone ( $P<0.05$ ). Within the endosteal region, the proximal host-allograft junction had more new bone than allograft sections ( $P<0.05$ )(Figure 12). Similarly, the mid-cortical region had more new bone in the proximal and distal host-allograft junctions than allograft sections ( $P<0.05$ ).

Treatment differences were evaluated for a given region and section (Table 8). New bone in the periosteal region had treatment differences in 2 of 3 sections evaluated. At the proximal host-allograft junction, treatments 'np' and 'npe' had more new bone than treatment 'ne' ( $P<0.05$ ). At the distal host-allograft junction, treatments 'np' and 'npe' had more new bone than treatment 'nc' ( $P<0.05$ ). There was no difference in periosteal new bone between treatments along the allograft. New bone in the mid-cortical region had treatment differences only at the proximal host-allograft junction. At this section, treatment 'npe' had more mid-cortical new bone than treatment 'ne' ( $P<0.05$ ). New bone in the endosteal region was variable, ranging from none to abundant. Consequently, only the distal host-allograft junction had adequate sample size for statistical analysis. At this section, treatment 'np' had more new bone than treatment 'ne' ( $P<0.05$ ).

## Discussion

Potential differences in limb function, remodeling activity, and allograft incorporation were evaluated for commonly available methods (autogenous cancellous bone and intramedullary cement) of augmenting allograft fixation in this *in vivo* canine model. Six months after surgery, differences between treatments, although present, were more subtle than expected. Before sacrifice, with the ILN fixation in place, there was no difference in physical activity evident between treatment groups. This time period was chosen to evaluate the healing process at an intermediary stage, before processes with the various treatments reached similar levels of healing.

Autogenous cancellous bone for fracture augmentation in dogs is typically harvested from the humerus, iliac crest, or tibia. In this canine allograft model, harvest of the allograft and reaming of the femur for ILN placement exposed good quantities of cancellous bone from the proximal and distal femur. A recent report by DeVries and associates evaluated the effect of different volumes of autogenous cancellous bone placed in an ulnar defect (7.5 x 6-mm).<sup>30</sup> They found that maximum bony ingrowth was obtained with 0.3 g autogenous cancellous bone. Quantities greater than this did not add increased benefit. In the study reported here, a mean of 0.5 g autogenous cancellous bone was added to the 4 groups receiving it. Although this quantity was divided between 2 or 3 locations, any gaps at the host-allograft junctions were less than 1-mm and the quantity applied to endosteal surfaces was limited by presence of the ILN.

The absence of differences in peak vertical ground reaction forces between treatments suggests that the overall gait differences recorded result as a consequence of the surgical procedure. The ILN fixation stabilized all treatments such that uniform levels of limb function were achieved. In a study by Markel and associates, comparing allograft/endoprosthesis components using step-cut and transverse osteotomies, dogs with transverse osteotomies had greater peak vertical ground reaction forces over 6 months.<sup>24</sup> The 4 week peak force values from those dogs were similar to the dogs with step-cut osteotomies in the study reported here. However, at 12 and 24 weeks after surgery, the step-cut osteotomy values from the study reported here were more similar to those with step-cut osteotomies in the previous study. Perhaps there is a functional advantage to using transverse osteotomies at host-allograft junctions.

Typical ILN fixation does not achieve compression across the host-allograft junctions. It seems probable that compression would result in better host-allograft contact and better allograft incorporation. Dynamic compression plates have the advantage of providing such compression. However, they also have the disadvantage of requiring screws to be placed through the allograft, increasing the risk of fracture. There are reports of new ILN techniques that allow compression.<sup>31</sup> Such devices warrant further investigation for use with segmental allografts. With standard ILN fixation, better host-allograft contact may potentially be obtained with transverse osteotomies rather than the step-cut osteotomies used in this study. Step-cut osteotomies provide rotational

stability for the graft, but it is difficult to achieve perfect contact of all host-allograft surfaces. Even so, a potential disadvantage of transverse osteotomies is the lack of rotational stability. Without adequate compression, rotation may occur, leading to increased motion of the graft.

Although values varied some by section and time, overall callus area, new bone formation and porosity were greatest in periosteal regions of treatments including autogenous cancellous bone applied to the periosteal surface (treatments 'ncp', 'np', and 'npe'). These differences were more apparent at host-allograft junctions than the allograft, suggesting the stimulus provided by the cancellous bone requires a host bone response. This same pattern did not hold true for new bone formation and porosity with endosteal regions in treatments including cancellous bone applied to the endosteal surface (treatments 'ne' and 'npe'). Insertion of the ILN may have dislodged the additional endosteal cancellous bone or it may be a mechanistic difference, as other investigators have observed decreased endosteal callus area and new bone in allograft segments compared to adjacent host bone.<sup>32</sup> None of the treatments yielded substantially improved properties for mid-cortical regions of the central allograft. This is typical for what has been reported with the central allograft for other treatments, as well.<sup>21,33</sup>

Supplementation of allografts with autogenous cancellous bone at the host-allograft junction has been reported to decrease the time for bone union in human patients from 15 to 8 months.<sup>15</sup> Although there were differences between treatments in the study

reported here for the degree of union achieved, the most notable finding was that the group receiving intramedullary PMMA without additional cancellous bone (treatment 'nc') had the least amount of complete union, the poorest histologic scores, and the greatest gap remaining at 6 months. This suggests there was interference by the PMMA. Given time, all of these grafts may have eventually united. In contrast, the group receiving PMMA and cancellous bone (treatment 'ncp') had union, histologic scores, and remaining gap that were as good or better than other treatments. As was noted in the results, neither of these groups had histologic evidence of cement in the host-allograft interface. The apparent delay in union at 6 months with PMMA treatment by itself is in contrast to what Straw and associates observed at 9 months in the dog with a plated allograft model using intramedullary PMMA.<sup>12</sup> There would appear to be greater risk of pushing the PMMA across the host-allograft junction with an ILN technique. A pilot study applying plates and PMMA to human patients also observed a non-union rate greater than that of Straw and associates.<sup>13</sup> Evaluation of allografts retrieved from human patients with intramedullary fixation and intramedullary PMMA showed no evidence of resorption adjacent to the graft.<sup>21</sup> However, there also was no revascularization or tissue ingrowth of the allograft adjacent to the cement. This same report suggested that immature union may take place despite radiographic evidence of a radiolucent line. In cases of radiographic non-union without other confirming signs, the recommendation was to continue observation rather than intervening immediately.

There were no differences in bone mineral density between treatments throughout the study reported here. The general changes in BMD observed between pre-operative scans and immediately post-operative have been described before as an implant-related event.<sup>25,34</sup> The femoral head region was chosen as a reference site removed from the implant. Immediate post-operative BMD for this region was not different from pre-surgery values. Over time, however, all dogs lost BMD from this region. This loss in BMD may have been related to the relative inactivity of the dogs over the study period.

The results of this study suggest that augmentation of ILN stabilized allografts with intramedullary PMMA by itself has negative effects on bone union, residual gap, and tissue type at the host-allograft junction. Of the 6 treatments evaluated, comparing all properties, the greatest gain overall was obtained with ILN fixation augmented by (1) intramedullary PMMA and autogenous cancellous bone at the host-allograft junction or (2) a combination of autogenous cancellous bone packed in the medullary canal and applied to the host-allograft junction.

**Acknowledgments:** This publication was supported by the Department of the Navy (grant no. N00014-93-1-0745), National Institute on Aging (grant no. 1 T32 AG00213) and the National Institute of Arthritis, Musculoskeletal and Skin Diseases (grant no. 1 F32 AR08340). The authors thank Dr. Kei Hayashi, Dr. Chris Murphy, Kathy Massa, Janet Neickarz, Jessica Steichen, and Lyndsey Yoshino for assistance with performing surgeries, radiographic callus area determination, and mixed lymphocyte culture assays.

### References

1. Friedlaender G: Bone grafts: The basic science rationale for clinical applications. *J Bone Joint Surg [Am]* 69-A:786-790, 1987.
2. Innis P, Randolph M, Paskert J, et al: Vascularized bone allografts: in vitro assessment of cell-mediated and humoral responses. *Plast Reconstr Surg* 87:315-325, 1991.
3. Phillips J, Rahn B: Fixation effects on membranous and endochondral onlay bone graft revascularization and bone deposition. *Plast Reconstr Surg* 85:891-897, 1990.
4. Stevenson S: The immune response to osteochondral allografts in dogs. *J Bone Joint Surg [Am]* 69-A:573-582, 1987.
5. Berrey B, Lord C, Gebhardt MC, Mankin HJ: Fractures of allografts. *J Bone Joint Surg [Am]* 72-A:825-833, 1990.
6. McDonald D, McGuire M: Complications of large fragment allografts. In: **Complications of Limb Salvage**, ed by K Brown, Montreal, ISOLS, 1992, pp 25-28.
7. Wippermann B, Zwipp H, Junge P, et al: Healing of a segmental defect in the sheep tibia filled with a hydroxyapatite ceramic (HA) augmented by basic fibroblast growth factor (bFGF) and autologous bone marrow. *Trans ORS* 19:5451994.
8. Mankin HJ, Gebhardt MC, Jennings LC, Springfield DS, Tomford WW: Long-term results of allograft replacement in the management of bone tumors. *Clin Orthop* 324:86-97, 1996.

9. Harrington KD, Johnston JO, Turner RH, Green DL: The use of methylmethacrylate as an adjunct in the internal fixation of malignant neoplastic fractures. *J Bone Joint Surg [Am]* 54-A:1665-1676, 1972.
10. Harrington KD: The use of methylmethacrylate as an adjunct in the internal fixation of unstable comminuted intertrochanteric fractures in osteoporotic patients. *J Bone Joint Surg [Am]* 57-A:744-750, 1975.
11. Harrington KD, Sim FH, Enis JE, Johnston JO, Dick HM, Gristina AG: Methylmethacrylate as an adjunct in internal fixation of pathological fractures. *J Bone Joint Surg [Am]* 58-A:1047-1055, 1976.
12. Straw R, Powers B, Withrow S, Cooper MF, Turner AS: The effect of intramedullary polymethylmethacrylate on healing of intercalary cortical allografts in a canine model. *J Orthop Res* 10:434-439, 1992.
13. Wunder JS, Davis AM, Hummel JS, Mandelcorn J, Griffin AM, Bell RS: The effect of intramedullary cement on intercalary allograft reconstruction of bone defects after tumour resection: a pilot study. *Can J Surg* 38:521-527, 1995.
14. Roush JK, Wilson JW: Effects of plate luting on cortical vascularity and development of cortical porosity in canine femurs. *Vet Surg* 19:208-214, 1990.
15. Wang J, -W., Shih C, -H. Allograft transplantation in aggressive or malignant bone tumors. *Clin Orthop* 297:203-209, 1993.

16. Alexander JW: Use of a combination of cortical bone allografts and cancellous bone autografts to replace massive bone loss in fresh fractures and selected nonunions. *J Am Anim Hosp Assoc* 19:671-678, 1983.
17. Johnson AL: Principles and practical application of cortical-bone grafting techniques. *Comp Cont Educ Pract Vet* 10:906-913, 1988.
18. Cara JA, Lacleriga A, Canadell J: Intercalary bone allografts: 23 tumor cases followed for 3 years. *Acta Orthop Scand* 65:42-46, 1994.
19. Kienapfel H, Sumner D, Turner T, et al: Efficacy of autograft and freeze-dried allograft to enhance fixation of porous coated implants in the presence of interface gaps. *J Orthop Res* 10:423-433, 1992.
20. Koskinen E: Wide resection of primary tumors of bone and replacement with massive bone grafts: An improved technique for transplanting allogeneic bone grafts. *Clin Orthop* 134:302-319, 1978.
21. Enneking WF, Mindell ER: Observations on massive retrieved human allografts. *J Bone Joint Surg [Am]* 73-A:1123-1142, 1991.
22. Schweiberer L, Stutzle H, Mandelkow H: Bone transplantation. *Acta Orthop Trauma Surg* 109:1-8, 1989.
23. Budsberg SC, Jevens DJ, Brown J, Foutz TL, DeCamp CE, Reece L: Evaluation of limb symmetry indices, using ground reaction forces in healthy dogs. *Am J Vet Res* 54:1569-1574, 1993.

24. Markel MD, Wood SA, Bogdanske JJ, Rapoff AJ, Kalscheur VL, Bouvy BM, Rock MG, Chao EY, Vanderby R, Jr. Comparison of healing of allograft/endoprosthesis composites with three types of gluteus medius attachment. *J Orthop Res* 13:105-114, 1995.
25. Markel MD, Bogdanske JJ: Dual-energy X-ray absorptiometry of canine femurs with and without fracture fixation devices. *Am J Vet Res* 55:862-866, 1994.
26. Hanson PD, Warner C, Vanderby R, Jr., Frassica DA, Markel MD: The effect of autogenous cancellous bone and intramedullary cement on allograft strength. *Submitted to J Biomech* 1997.
27. **Methods of Calcified Tissue Preparation.** Amsterdam, Elsevier, 1984.
28. Villanueva AR: Bone. In: **Theory and Practice of Histotechnology**, ed by DC Sheehan, BB Hrapchak, Columbus, Battelle Press, 1980, pp 89-117.
29. Burwell RG: Studies in the transplantation of bone. VIII. Treated composite homografts of cancellous bone: an analysis of inductive mechanisms in bone transplantation. *J Bone Joint Surg [Br]* 48-B:532-566, 1964.
30. DeVries WJ, Runyon CL, Martinez SA, Ireland WP: Effect of volume variations on osteogenic capabilities of autogenous cancellous bone graft in dogs. *Am J Vet Res* 57:1501-1505, 1996.

31. Durall I, Diaz MC, Morales I: An experimental study of compression of femoral fractures by an interlocking intramedullary pin. *V C O T* 6:93-99, 1993.
32. Muir P, Johnson KA: Tibial intercalary allograft incorporation: comparison of fixation with locked intramedullary nail and dynamic compression plate. *J Orthop Res* 13:132-137, 1995.
33. Enneking WF, Burchardt H, Puhl JJ, Piotrowski G: Physical and biological aspects of repair in dog cortical bone transplants. *J Bone Joint Surg [Am]* 57-A:232-236, 1975.
34. Muir P, Markel MD, Bogdanske JJ, Johnson KA: Dual-energy x-ray absorptiometry and force-plate analysis of gait in dogs with healed femora after leg-lengthening plate fixation. *Vet Surg* 24:15-24, 1995.

**Table 1.** Overall treatment distribution and by dog groups for surgery.**Overall Distribution**

Abbreviation	Treatment	Number	Number Evaluated
n	ILN, no adjunctive treatment	11	11
nc	ILN plus intramedullary PMMA within allograft	11	10
npc	ILN plus intramedullary PMMA and autogenous cancellous graft added to periosteal surface	6	5
ne	ILN plus autogenous cancellous graft within allograft medullary canal	7	7
np	ILN plus autogenous cancellous graft added to periosteal surface	7	7
npe	ILN plus autogenous cancellous graft added to periosteal surface and within allograft medullary canal	6	6

**Dog Groupings**

Group	Limb 1 Treatment	Limb 2 Treatment	Number of Dogs
1	n	nc	5
2	n	npe	6
3	ne	np	7
4	nc	npc	6

See Methods for details on randomization. ILN – interlocking nail.

**Table 2.** Autogenous cancellous bone harvested and applied to treatments.

<b>Treatment</b>	<b>Quantity (g)</b>
ncp	0.55 ± 0.05
ne	0.49 ± 0.02
np	0.55 ± 0.06
npe	0.42 ± 0.03

Values are the mean ± SEM for each treatment group. The total quantity of cancellous bone was divided equally between the sites (endosteal and periosteal, proximal and distal) it was applied.

Table 3. Callus area and change in allograft size over time.

Treatment	Total Callus Area (mm <sup>2</sup> )				Change in Allograft Size (mm <sup>2</sup> )	
	Lateral	Medial	Cranial	Caudal	Cranio-caudal View	Mediolateral View
<b>4 Weeks Post-Surgery</b>						
n	14.8 ± 2.8 <sup>C</sup>	24.3 ± 6.5	30.2 ± 8.3 <sup>BC</sup>	10.9 ± 5.4	46.9 ± 24.0	21.0 ± 4.8
nc	15.8 ± 2.6 <sup>C</sup>	29.5 ± 4.3	17.9 ± 3.4 <sup>C</sup>	19.0 ± 2.3	55.5 ± 29.4	14.8 ± 1.7
ncp	51.0 ± 8.6 <sup>AB</sup>	16.5 ± 4.8	55.8 ± 26.7 <sup>AB</sup>	44.9 ± 11.3	50.3 ± 11.3	39.2 ± 6.1
ne	20.0 ± 5.5 <sup>C</sup>	23.4 ± 6.9	33.9 ± 4.4 <sup>ABC</sup>	22.6 ± 6.6	17.3 ± 2.2	12.5 ± 9.5
np	59.5 ± 13.7 <sup>A</sup>	37.2 ± 14.4	46.0 ± 10.6 <sup>ABC</sup>	37.6 ± 17.6	53.1 ± 13.4	25.9 ± 13.7
npe	32.5 ± 7.6 <sup>BC</sup>	27.0 ± 5.8	63.2 ± 8.0 <sup>A</sup>	28.1 ± 14.2	33.1 ± 9.4	31.5 ± 12.2
<b>12 Weeks Post-Surgery</b>						
n	37.7 ± 12.4	34.7 ± 10.7	57.8 ± 27.0	36.8 ± 9.8	83.2 ± 37.9	52.5 ± 22.2
nc	36.6 ± 10.5	46.5 ± 13.0	66.1 ± 18.4	39.5 ± 13.7	91.0 ± 34.5	35.5 ± 11.2
ncp	46.4 ± 11.5	26.6 ± 16.1	105.5 ± 43.9	58.7 ± 18.9	61.8 ± 27.8	92.8 ± 27.9
ne	37.8 ± 9.2	47.2 ± 6.8	95.8 ± 22.4	69.3 ± 30.3	66.0 ± 14.6	94.5 ± 46.3
np	93.9 ± 27.5	65.8 ± 15.4	114.9 ± 29.5	100.2 ± 33.4	129.7 ± 60.5	96.1 ± 40.5
npe	63.3 ± 13.1	35.0 ± 8.6	99.6 ± 16.3	66.7 ± 24.3	73.3 ± 16.6	87.3 ± 29.4

Values are the mean ± SEM for total callus area from the given surface or change in allograft size relative to area immediately post-surgery from radiographs performed at 4, 12, and 24 weeks after surgery. Superscript letters that differ within a column indicate a significant difference for that time period ( $P < 0.05$ ).

Table 3 (continued).

Treatment	Total Callus Area (mm <sup>2</sup> )				Change in Allograft Size (mm <sup>2</sup> )	
	Lateral	Medial	Cranial	Caudal	Craniocaudal View	Mediolateral View
<b>24 Weeks Post-Surgery</b>						
n	35.6 ± 14.1	28.8 ± 6.5	55.8 ± 20.5	41.3 ± 12.7 <sup>B</sup>	53.2 ± 37.1	48.4 ± 27.3
nc	28.3 ± 8.2	39.3 ± 11.5	61.4 ± 20.7	31.0 ± 8.9 <sup>B</sup>	70.3 ± 31.8	17.9 ± 15.1
nep	29.2 ± 4.3	42.0 ± 35.0	80.2 ± 26.2	117.8 ± 37.1 <sup>A</sup>	33.9 ± 27.5	96.5 ± 40.6
ne	41.5 ± 10.8	55.9 ± 16.0	55.7 ± 11.2	35.9 ± 14.2 <sup>B</sup>	32.2 ± 19.8	48.2 ± 27.7
np	60.0 ± 16.9	48.2 ± 10.3	143.0 ± 32.5	119.2 ± 28.8 <sup>A</sup>	107.0 ± 43.6	106.2 ± 37.7
npe	38.2 ± 10.5	30.3 ± 7.5	74.2 ± 15.4	68.4 ± 23.6 <sup>AB</sup>	48.8 ± 19.0	84.3 ± 32.1

**Table 4.** Bone mineral density of allograft constructs at day 0, 12 weeks, and 24 weeks after transplantation.

Region and Treatment	Day 0 BMD (g/cm <sup>2</sup> )	12 Week BMD (g/cm <sup>2</sup> )	24 Week BMD (g/cm <sup>2</sup> )
<b>Global - entire field</b>			
n	0.786 ± .029 >	0.702 ± .018 ↓	0.701 ± .02 ↓
nc	0.805 ± .022 >	0.699 ± .025 ↓	0.698 ± .03 ↓
ncp	0.963 ± .151	0.725 ± .024	0.731 ± .01
ne	0.914 ± .040 >	0.763 ± .020 ↓	0.715 ± .02 ↓
np	0.858 ± .032 >	0.795 ± .015	0.779 ± .02
npe	0.809 ± .035 >	0.690 ± .026 ↓	0.696 ± .02 ↓
<b>R1 - length of nail</b>			
n	0.733 ± .039 >	0.663 ± .063	0.736 ± .04
nc	0.739 ± .025 >	0.752 ± .034	0.736 ± .03
ncp	0.798 ± .064 >	0.755 ± .042	0.766 ± .04
ne	0.808 ± .047 >	0.811 ± .025	0.774 ± .04
np	0.756 ± .037 >	0.792 ± .034	0.820 ± .02 †
npe	0.760 ± .050 >	0.738 ± .036	0.757 ± .04
<b>R2 - proximal host</b>			
n	0.786 ± .044 >	0.731 ± .044 ↓	0.771 ± .04
nc	0.785 ± .021 >	0.786 ± .033	0.777 ± .03
ncp	0.865 ± .097	0.819 ± .040	0.820 ± .05
ne	0.839 ± .073 >	0.820 ± .038 ↓	0.783 ± .06
np	0.800 ± .040 >	0.778 ± .052	0.822 ± .03
npe	0.815 ± .059 >	0.762 ± .042	0.790 ± .05
<b>R3 - proximal host-allograft junction</b>			
n	0.716 ± .058	0.704 ± .054	0.712 ± .05
nc	0.710 ± .044	0.694 ± .048	0.690 ± .03
ncp	0.802 ± .061	0.858 ± .065	0.825 ± .06
ne	0.844 ± .077	0.798 ± .076	0.776 ± .08
np	0.782 ± .058	0.760 ± .041	0.849 ± .03
npe	0.800 ± .069	0.748 ± .053	0.804 ± .08

Data are the mean ± SEM for treatments at each region of interest (Figure). Symbols indicate a significant difference ( $P < 0.05$ ) as follows: > - day 0 post-operative BMD greater than pre-operative value, < - day 0 post-operative BMD less than pre-operative value, † - 12 or 24 week BMD greater than day 0 value, ↓ - 12 or 24 week BMD less than day 0 value. See Table 1 for treatment abbreviations.

Table 4 (continued).

Region and Treatment	Day 0 BMD (g/cm <sup>2</sup> )	12 Week BMD (g/cm <sup>2</sup> )	24 Week (g/cm <sup>2</sup> )
<b>R4 - allograft</b>			
n	0.596 ± .027 <	0.529 ± .036 ↓	0.530 ± .05 ↓
nc	0.585 ± .026 <	0.538 ± .047	0.577 ± .05
ncp	0.557 ± .070	0.577 ± .042	0.595 ± .03
ne	0.670 ± .046	0.481 ± .106	0.604 ± .05
np	0.502 ± .090	0.505 ± .089	0.568 ± .04
npe	0.645 ± .031	0.650 ± .045	0.623 ± .04
<b>R5 - distal host-allograft junction</b>			
n	0.737 ± .052	0.744 ± .054	0.690 ± .05 ↓
nc	0.765 ± .059 >	0.731 ± .052	0.713 ± .03
ncp	0.855 ± .076 >	0.841 ± .061	0.810 ± .07
ne	0.803 ± .064	0.707 ± .056 ↓	0.736 ± .06
np	0.761 ± .073	0.793 ± .062	0.897 ± .03 †
npe	0.735 ± .068	0.774 ± .058	0.799 ± .06
<b>R6 - distal host</b>			
n	0.666 ± .036 >	0.714 ± .025	0.726 ± .04
nc	0.666 ± .041 >	0.732 ± .039	0.693 ± .03
ncp	0.703 ± .042 >	0.649 ± .044	0.693 ± .05
ne	0.802 ± .053 >	0.840 ± .034	0.813 ± .03
np	0.725 ± .056	0.851 ± .019	0.843 ± .05
npe	0.669 ± .040 >	0.725 ± .036 †	0.724 ± .03
<b>R7 - femoral head</b>			
n	0.981 ± .032	0.795 ± .038 ↓	0.873 ± .04 ↓
nc	1.090 ± .055	0.856 ± .056 ↓	0.907 ± .04 ↓
ncp	1.209 ± .145	0.902 ± .054 ↓	0.909 ± .04 ↓
ne	1.065 ± .029	0.885 ± .029 ↓	0.828 ± .02 ↓
np	1.064 ± .047	0.878 ± .026 ↓	0.900 ± .03 ↓
npe	1.010 ± .048	0.848 ± .031 ↓	0.875 ± .03

Table 5. Bone porosity of treatments at different regions and sections.

Treatment	Bone Porosity (%) of Section				
	Proximal Host	Proximal Host-Allograft Junction	Allograft	Distal Host-Allograft Junction	Distal Host
<b>New Periosteal Bone</b>					
n	13.7 ± 2.8	11.7 ± 2.0 <sup>B</sup>	9.6 ± 2.7 <sup>B</sup>	19.0 ± 3.7 <sup>AB</sup>	19.3 ± 7.0
nc	17.8 ± 3.1	18.5 ± 3.7 <sup>AB</sup>	15.7 ± 3.7 <sup>B</sup>	11.1 ± 2.2 <sup>B</sup>	14.5 ± 2.9
ncp	16.7 ± 4.6	12.9 ± 2.7 <sup>AB</sup>	11.2 ± 3.0 <sup>B</sup>	20.6 ± 6.2 <sup>AB</sup>	30.8 ± 11.2
ne	15.0 ± 5.1	11.8 ± 2.5 <sup>AB</sup>	11.3 ± 2.8 <sup>B</sup>	13.1 ± 2.8 <sup>B</sup>	20.7 ± 2.1
np	13.8 ± 3.4	15.5 ± 1.7 <sup>AB</sup>	16.0 ± 3.2 <sup>AB</sup>	14.9 ± 3.0 <sup>AB</sup>	11.9 ± 2.1
npe	12.5 ± 4.4	20.6 ± 4.4 <sup>A</sup>	25.9 ± 4.7 <sup>A</sup>	27.3 ± 7.4 <sup>A</sup>	25.1 ± 6.6
<b>Mid-Cortical Bone</b>					
n	3.9 ± 0.5	7.0 ± 1.4	7.0 ± 1.0 <sup>AB</sup>	8.6 ± 1.9	4.6 ± 1.1 <sup>AB</sup>
nc	7.6 ± 4.9	8.5 ± 1.5	8.5 ± 2.0 <sup>AB</sup>	7.8 ± 2.3	6.1 ± 1.2 <sup>AB</sup>
ncp	5.3 ± 1.6	6.2 ± 2.1	11.8 ± 4.6 <sup>A</sup>	14.4 ± 3.2	4.5 ± 0.9 <sup>AB</sup>
ne	5.5 ± 1.2	8.2 ± 2.8	4.7 ± 0.9 <sup>AB</sup>	7.2 ± 2.5	3.9 ± 1.2 <sup>B</sup>
np	3.4 ± 1.1	3.6 ± 0.9	2.9 ± 0.9 <sup>B</sup>	6.5 ± 2.2	5.8 ± 1.1 <sup>AB</sup>
npe	7.2 ± 2.8	6.9 ± 2.6	10.1 ± 2.6 <sup>A</sup>	8.3 ± 2.4	8.1 ± 2.2 <sup>A</sup>

Values are the mean ± SEM for treatments from the sections and regions indicated. See Table 1 for treatment abbreviations. For a given region, superscript letters that differ within a column indicate a significant difference between least-squares means of treatments ( $P < 0.05$ ).

Table 5 (continued).

Treatment	Proximal Host	Section Bone Porosity (%)			Distal Host
		Proximal Host-Allograft Junction	Allograft	Distal Host-Allograft Junction	
<b>New Endosteal Bone</b>					
n	38.8 ± 4.9 <sup>A</sup>	18.1 ± 4.8	31.5 ± 7.8	21.7 ± 5.8 <sup>AB</sup>	37.1 ± 4.0
nc	22.8 ± 2.1 <sup>B</sup>	13.8 ± 9.4	*	18.2 ± 5.6 <sup>AB</sup>	33.9 ± 5.9
nep	29.6 ± 6.0 <sup>AB</sup>	18.2 ± 11.8	12.2 ± 4.5	24.1 ± 13.2 <sup>AB</sup>	30.1 ± 8.4
ne	20.0 ± 3.2 <sup>B</sup>	26.0 ± 5.9	9.9 *	13.4 ± 3.4 <sup>B</sup>	33.1 ± 7.0
np	21.7 ± 6.9 <sup>B</sup>	30.1 ± 11.5	*	37.9 ± 6.0 <sup>A</sup>	29.6 ± 7.4
npe	37.9 ± 5.6 <sup>A</sup>	33.6 ± 6.9	23.7 ± 7.8	19.7 ± 8.8 <sup>AB</sup>	36.3 ± 5.2

\* - Treatments 'nc' and 'np' had insufficient new endosteal bone to evaluate within the allograft section.  
 Treatment 'ne' had only 1 observation at this location.

**Table 6.** Overall histologic score and mean gap by osteotomy location.

	Histologic Score (0-4)			Gap (mm)
	Bone	Fibrous	Cartilage	
Proximal Host-Allograft Junction	1.85 ± 0.12*	1.99 ± 0.13*	0.50 ± 0.06	0.83 ± 0.08*
Distal Host-Allograft Junction	2.51 ± 0.13*	1.43 ± 0.12*	0.32 ± 0.05	0.58 ± 0.07*

Values are the mean ± SEM histologic score (0=0%, 1=1-25%, 2=26-50%, 3=51-75%, 4=76-100%) or gap (mm) of all treatments and quadrants at the sections indicated. \* - Indicates a significant difference within a column between proximal and distal host-allograft junctions ( $P < 0.05$ ).

**Table 7.** Overall histologic score and mean gap by bone quadrant.

Quadrant	Histologic Score (0-4)			Gap (mm)
	Bone	Fibrous	Cartilage	
Lateral	2.45 ± 0.18 <sup>A</sup>	1.58 ± 0.18	0.33 ± 0.07 <sup>B</sup>	0.82 ± 0.13
Medial	2.37 ± 0.19 <sup>A</sup>	1.62 ± 0.19	0.19 ± 0.05 <sup>B</sup>	0.71 ± 0.12
Cranial	2.04 ± 0.17 <sup>B</sup>	1.68 ± 0.16	0.58 ± 0.09 <sup>A</sup>	0.64 ± 0.09
Caudal	1.84 ± 0.18 <sup>B</sup>	1.98 ± 0.18	0.54 ± 0.08 <sup>A</sup>	0.67 ± 0.08

Values are the mean ± SEM histologic score (0=0%, 1=1-25%, 2=26-50%, 3=51-75%, 4=76-100%) or gap (mm) of all treatments and quadrants at the sections indicated. Superscript letters that differ within a column indicate a significant difference between quadrants ( $P<0.05$ ).

**Table 8.** New bone formation of treatments at different regions and sections.

Treatment	Section New Bone (%)		
	Proximal Host-Allograft Junction	Allograft	Distal Host-Allograft Junction
<b>Periosteal Region</b>			
n	80.2 ± 3.6 <sup>AB</sup>	78.8 ± 3.1	77.1 ± 4.8 <sup>AB</sup>
nc	78.5 ± 3.4 <sup>AB</sup>	80.3 ± 6.4	70.0 ± 3.1 <sup>B</sup>
ncp	80.0 ± 3.9 <sup>AB</sup>	77.4 ± 4.2	84.6 ± 3.8 <sup>AB</sup>
ne	68.9 ± 4.0 <sup>B</sup>	76.5 ± 5.0	81.7 ± 5.0 <sup>AB</sup>
np	88.1 ± 3.3 <sup>A</sup>	79.4 ± 5.2	87.9 ± 3.0 <sup>A</sup>
npe	88.5 ± 5.2 <sup>A</sup>	87.7 ± 8.1	86.5 ± 5.3 <sup>A</sup>
<b>Mid-Cortical Region</b>			
n	45.8 ± 4.5 <sup>AB</sup>	32.2 ± 4.0	51.9 ± 4.3
nc	38.8 ± 4.6 <sup>AB</sup>	30.6 ± 4.0	36.6 ± 4.7
ncp	35.8 ± 5.5 <sup>AB</sup>	27.4 ± 3.4	51.9 ± 5.2
ne	31.1 ± 4.7 <sup>B</sup>	28.3 ± 3.8	34.1 ± 4.7
np	35.7 ± 5.3 <sup>AB</sup>	18.6 ± 4.1	46.1 ± 5.9
npe	54.7 ± 5.4 <sup>A</sup>	26.7 ± 4.4	47.8 ± 4.5
<b>Endosteal Region</b>			
n	85.3 ± 6.9	65.7 ± 5.6	76.7 ± 6.0 <sup>AB</sup>
nc	81.3 ± 37.7	*	73.9 ± 6.8 <sup>AB</sup>
ncp	78.5 ± 7.4	53.3 *	64.3 ± 11.7 <sup>AB</sup>
ne	75.2 ± 8.1	52.8 ± 8.2	54.4 ± 8.7 <sup>B</sup>
np	99.5 ± 14.6	*	90.5 ± 11.7 <sup>A</sup>
npe	84.2 ± 6.6	58.9 ± 8.2	75.3 ± 10.1 <sup>AB</sup>

Values are the mean ± SEM for treatments from the sections and regions indicated. See Table 1 for treatment abbreviations. For a given region, superscript letters that differ within a column indicate a significant difference between least-squares means of treatments ( $P < 0.05$ ). \* - Treatments 'nc' and 'np' had insufficient new endosteal bone to evaluate within the allograft section. Treatment 'ne' had only 1 observation at this location.

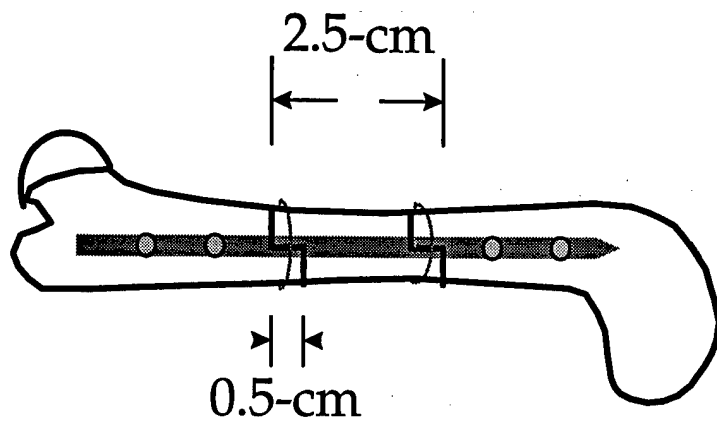


**Figure 1.** Illustration depicting placement of interlocking nail (ILN) in the femur to stabilize the mid-diaphyseal allograft. All treatments received an ILN with 2.7-mm screws placed proximal and distal to the allograft through the host bone. Single cerclage wires were placed at each step-cut osteotomy.

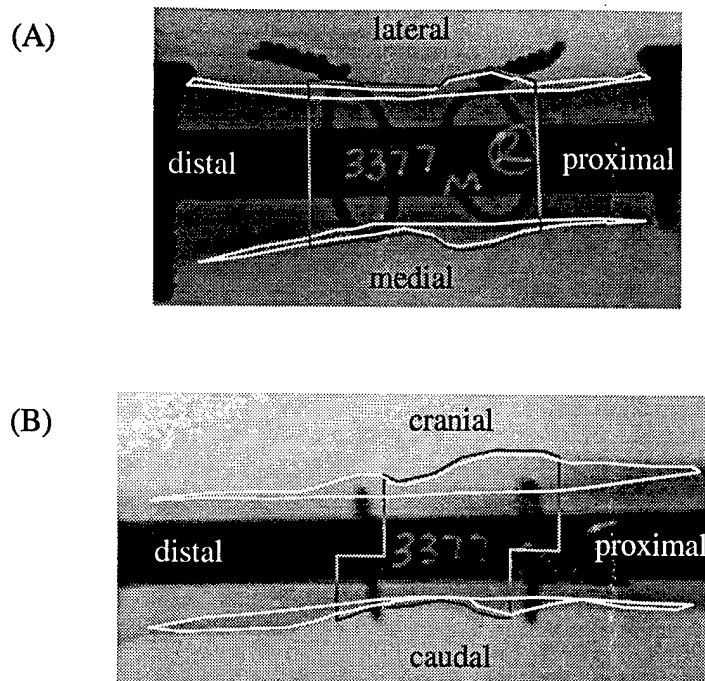


**Figure 2.** Example of regions evaluated for callus area (white outlines) and allograft area (gray outlines) from radiographic images. (A) Craniocaudal view highlights lateral and medial bone surfaces. (B) Mediolateral view highlights cranial and caudal bone surfaces. The images were inverted for better contrast with printing. Callus and allograft area were determined from 4, 12, and 24 week images. Allograft area was compared to that immediately post-surgery to determine the change in allograft size.

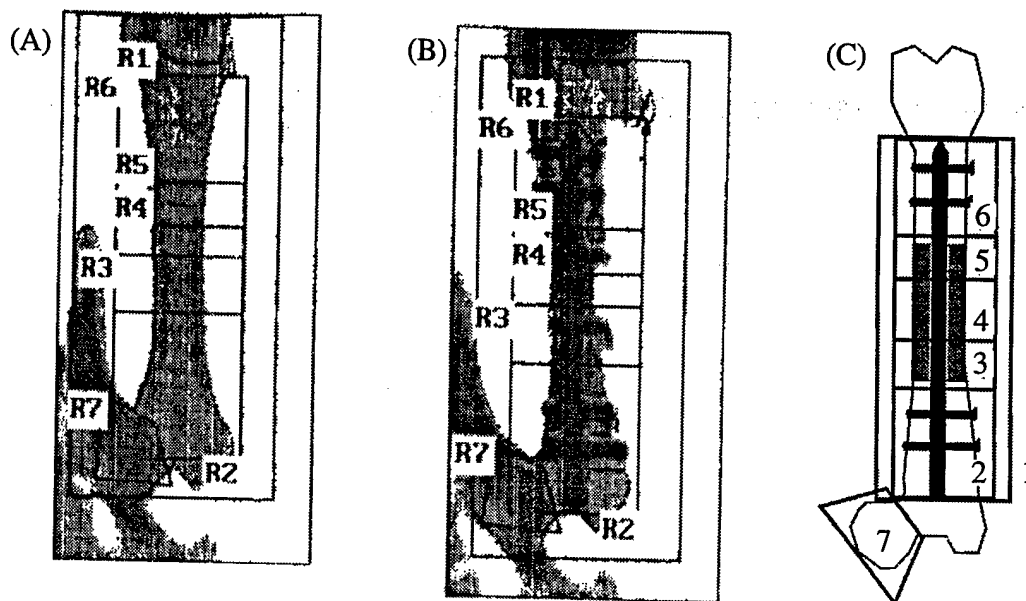


**Figure 3.** Illustrations of regions of interest evaluated for bone mineral density from craniocaudal DXA scans: (A) pre-operative image, (B) day 0 post-operative image, and (C) line drawing to emphasize regions of interest. The proximal aspect of the femur is towards the bottom of the illustration and the distal aspect is towards the top. A portion of the pelvis is visible along the bottom left. Regions of interest were selected using the day 0 post-operative scan and then applied to the pre-operative, 12 week, and 24 week scans to ensure consistency. Regions of interest: Global - entire femur (largest inner rectangle), R1 - femur along length of ILN, R2 - proximal host bone, R3 - proximal host-allograft junction, R4 - allograft bone, R5 - distal host-allograft junction, R6 - distal host bone, R7 - femoral head. The above images were taken from the printed output of the Hologic QDR-1000/W DXA unit. Actual image quality used for analysis was comparable to a standard radiograph.

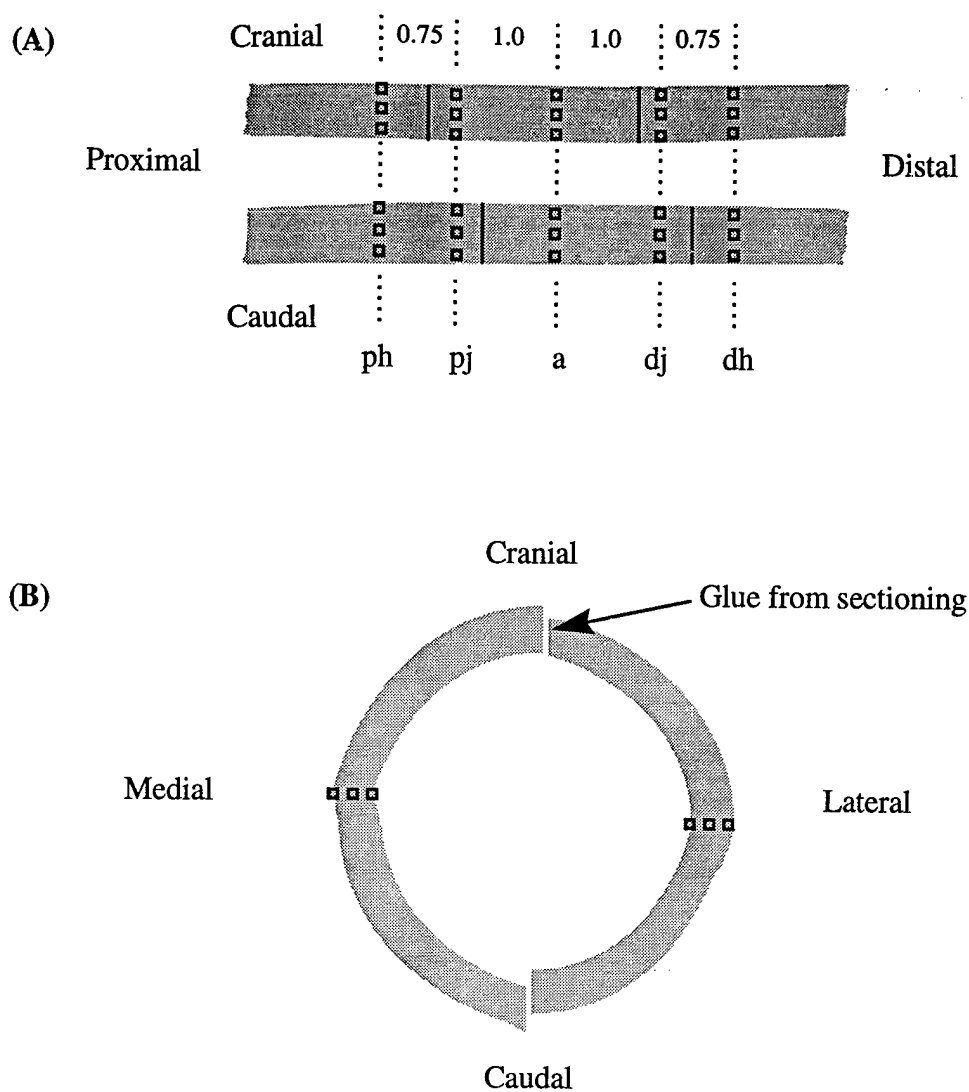


**Figure 4.** Illustrations of (A) sagittal and (B) transverse sections evaluated for porosity and new bone formation. Osteotomy sites are depicted by solid lines. Sagittal sections (100- $\mu$ m) were used to measure parameters at 3 regions of interest (new periosteal bone, mid-cortical bone, and new endosteal bone; depicted by boxes above) of the cranial and caudal cortices at each of the 5 locations indicated: ph—proximal host, pj—proximal host-allograft junction, a—allograft, dj—distal host-allograft junction, and dh—distal host. After gluing the resulting bone halves together, transverse sections (100- $\mu$ m) were taken at each of the 5 locations indicated (numbers indicate distance (cm) between locations). The 3 regions of interest from the medial and lateral cortices were then evaluated for each location.

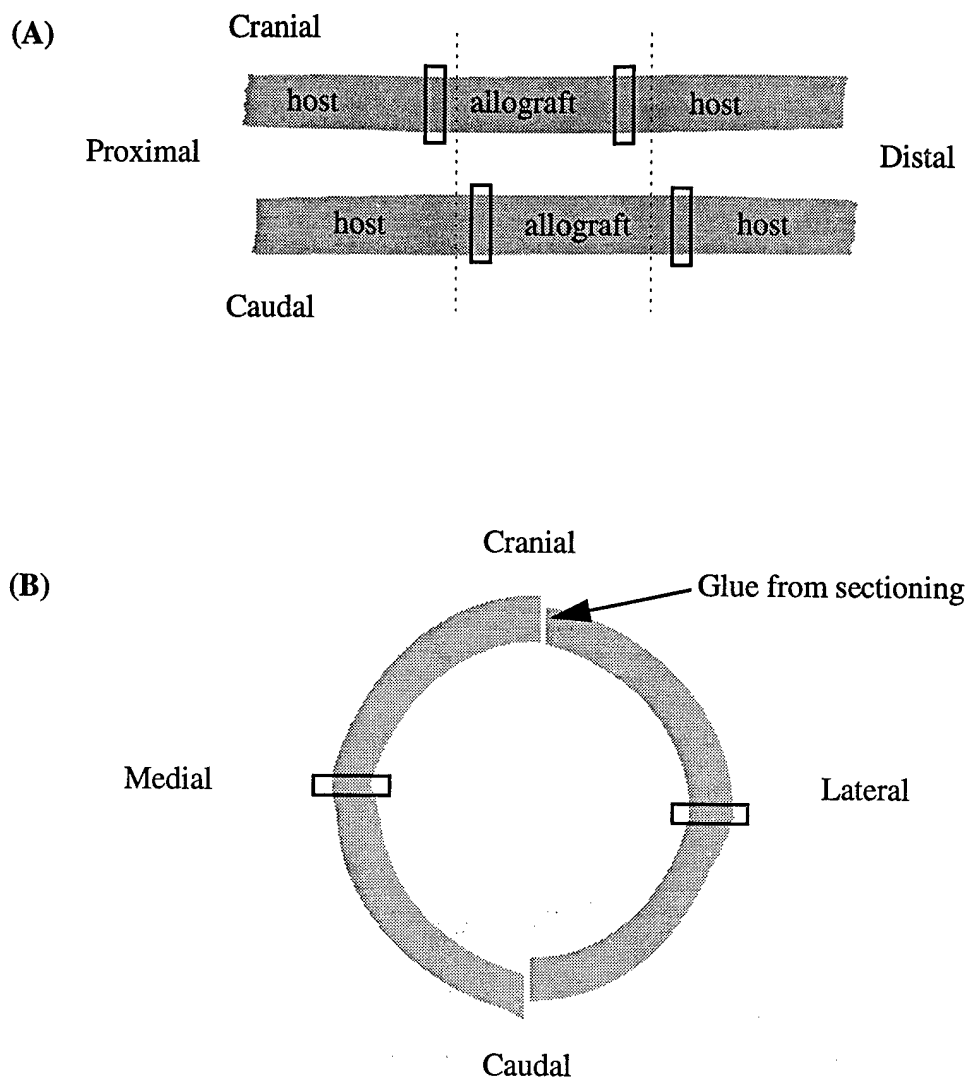


**Figure 5.** Illustrations depicting (A) sagittal and (B) transverse sections used to evaluate tissue histologic scoring and gap size at proximal and distal host-allograft junctions (boxes indicate osteotomy zones evaluated). Dotted lines on sagittal illustration indicate where transverse sections were taken. With transverse sections, proximal junctions had allograft in the cranial portion and host bone in the caudal portion. Whereas distal junctions had host bone in the cranial portion and allograft in the caudal portion.

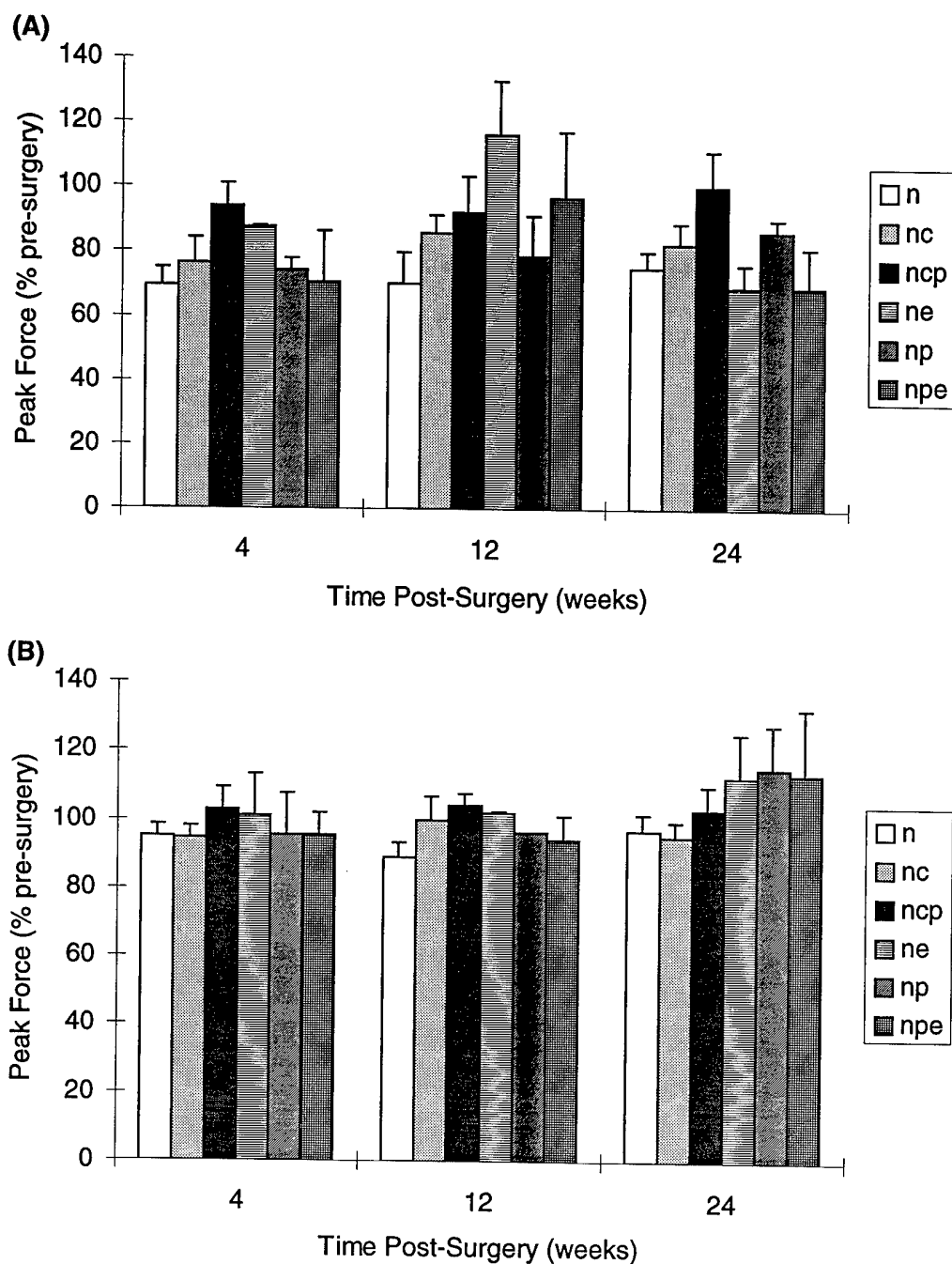


**Figure 6.** Peak vertical ground reaction force for (A) treated rear limbs and (B) corresponding fore limbs expressed as the percent of pre-surgery values. Values are the mean  $\pm$  SEM. There was no significant difference between treatments.

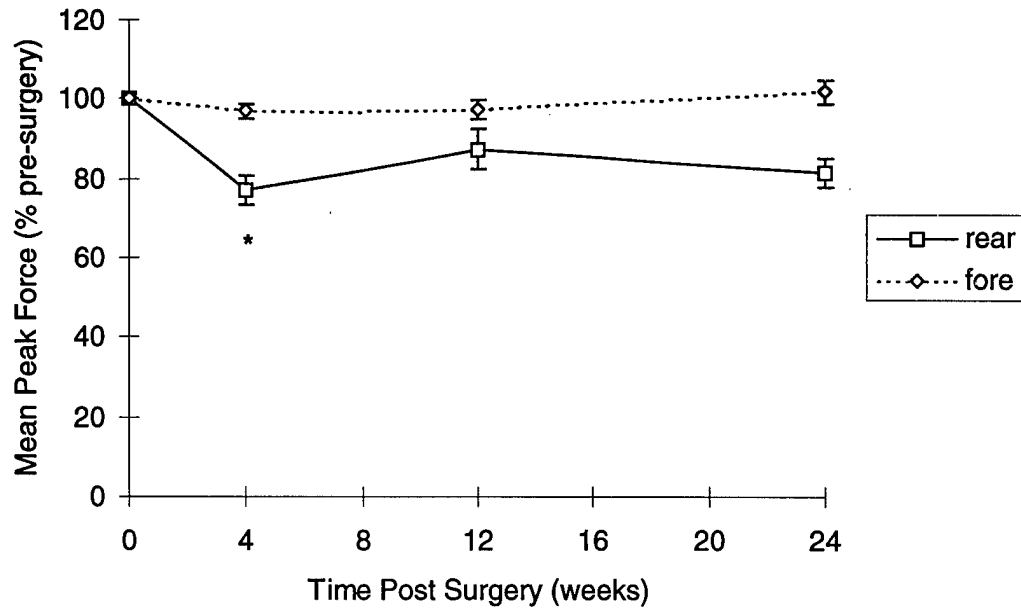


**Figure 7.** Mean peak vertical reaction force from all treatments for treated rear limb and untreated fore limb. Force is expressed as the percent of pre-surgery values (mean  $\pm$  SEM). \* - Indicates a significant difference between rear limb force at that time point and pre-surgery value ( $P < 0.05$ ).

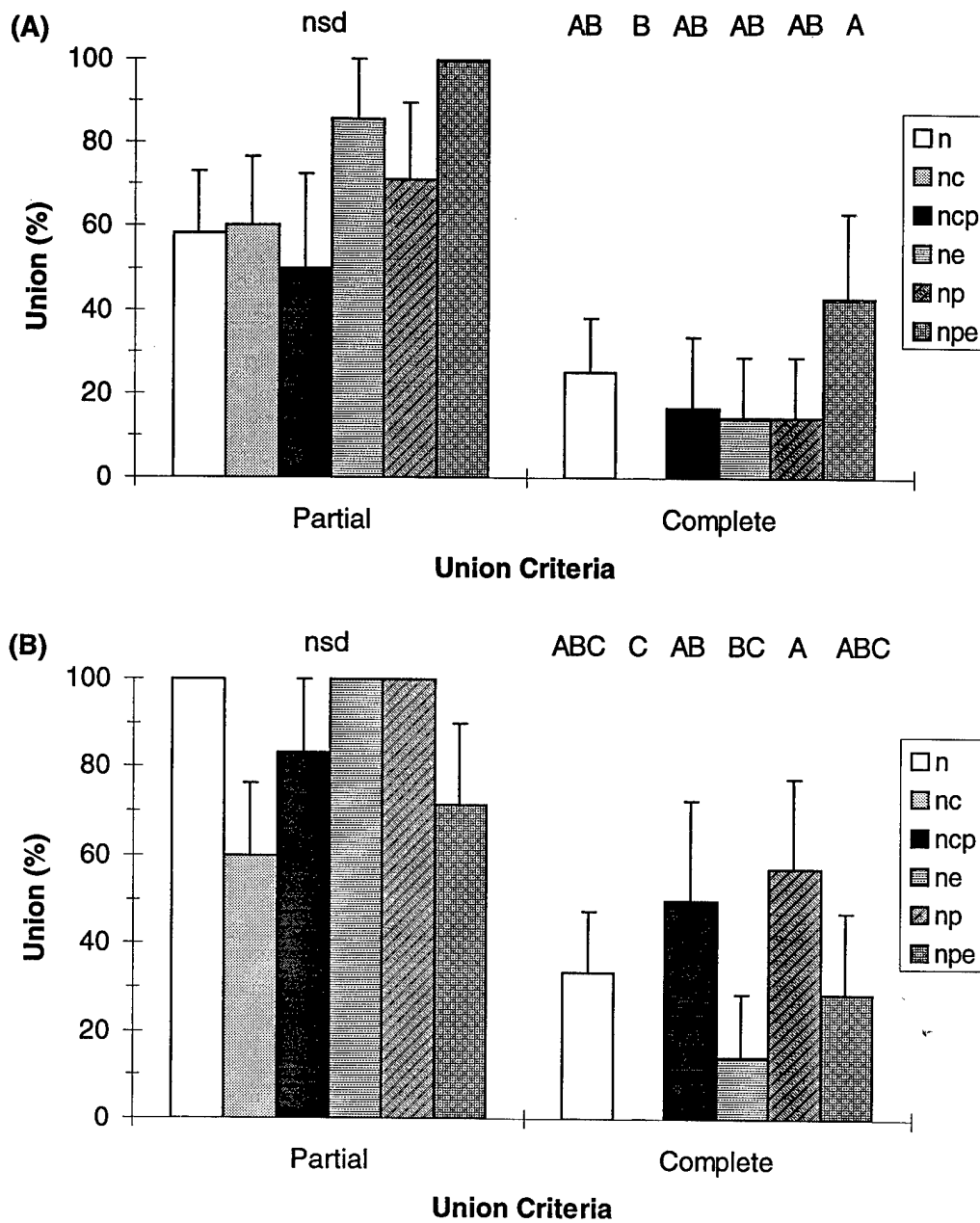


**Figure 8.** The percent of bony union determined from microradiographs for (A) the proximal host-allograft junction and (B) the distal host-allograft junction. Values are the mean  $\pm$  SEM from treatments at each osteotomy. Superscript letters above columns that differ indicate significance based on the given union definition ( $P < 0.05$ ). nsd – no significant difference.

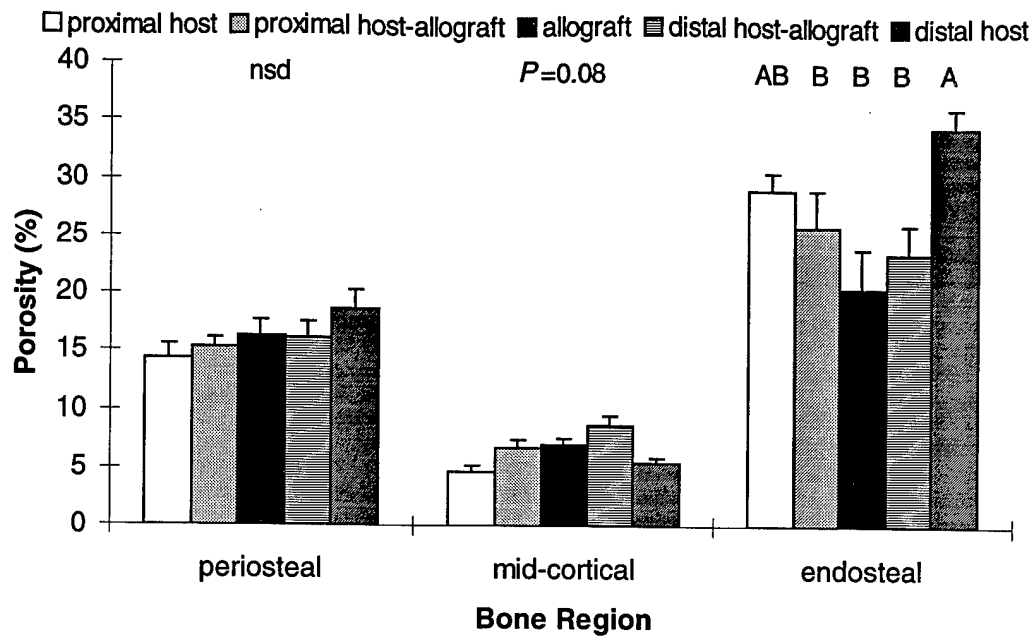


**Figure 9.** Overall bone porosity (mean  $\pm$  SEM) of cortical regions determined from microradiographs of sections from all treatments. See Table 4 for treatment differences at each region and section. Letters above columns that differ indicate significance between section locations within that region ( $P < 0.05$ ). nsd – no significant difference.

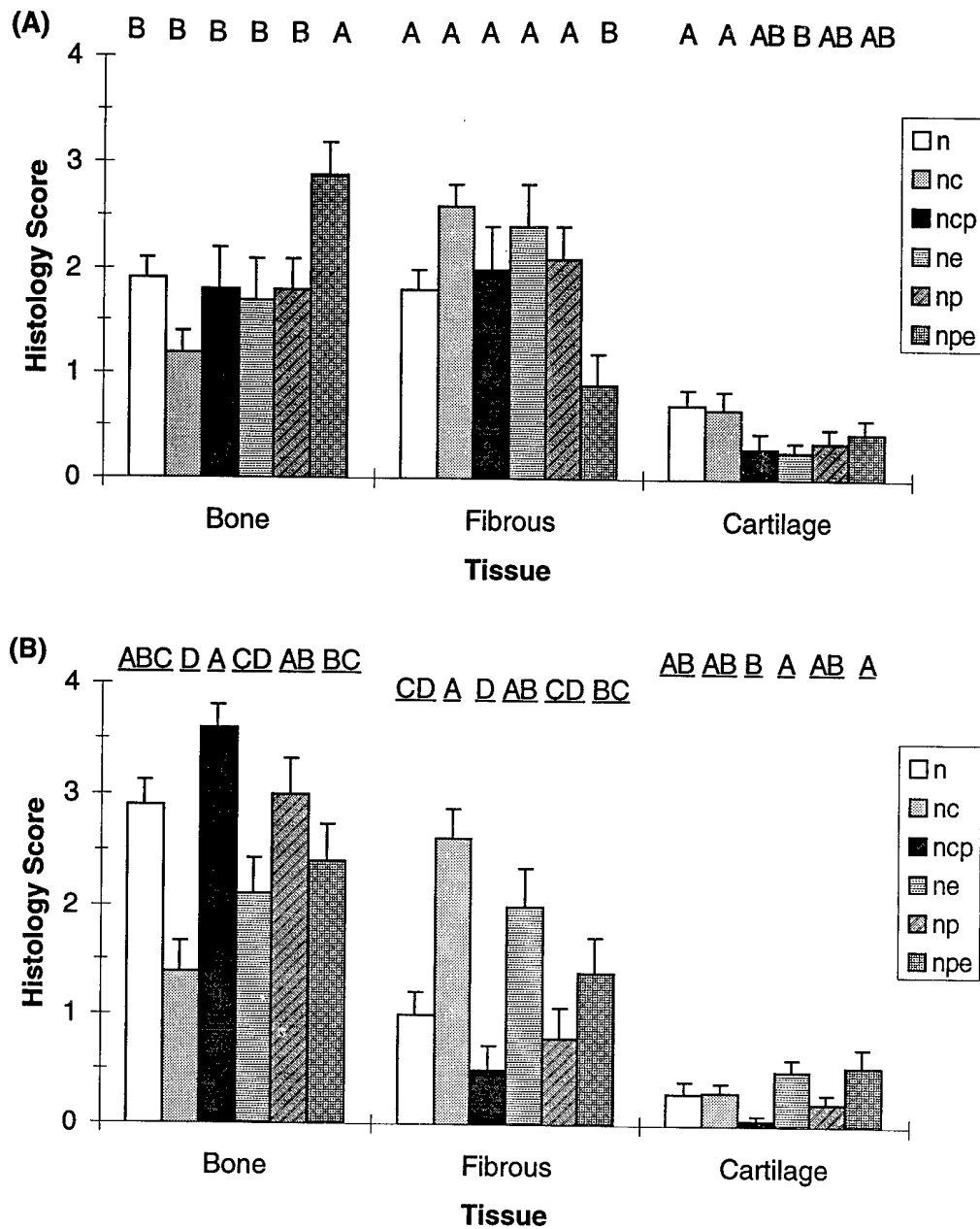


**Figure 10.** Histology score of tissues at (A) the proximal host-allograft junction and (B) the distal host-allograft junction (mean  $\pm$  SEM of all quadrants from each treatment). Tissue was scored as follows: 0=0%, 1=1-25%, 2=26-50%, 3=51-75%, and 4=76-100%. Letters that differ above columns indicate a significant difference within that tissue type ( $P < 0.05$ ).

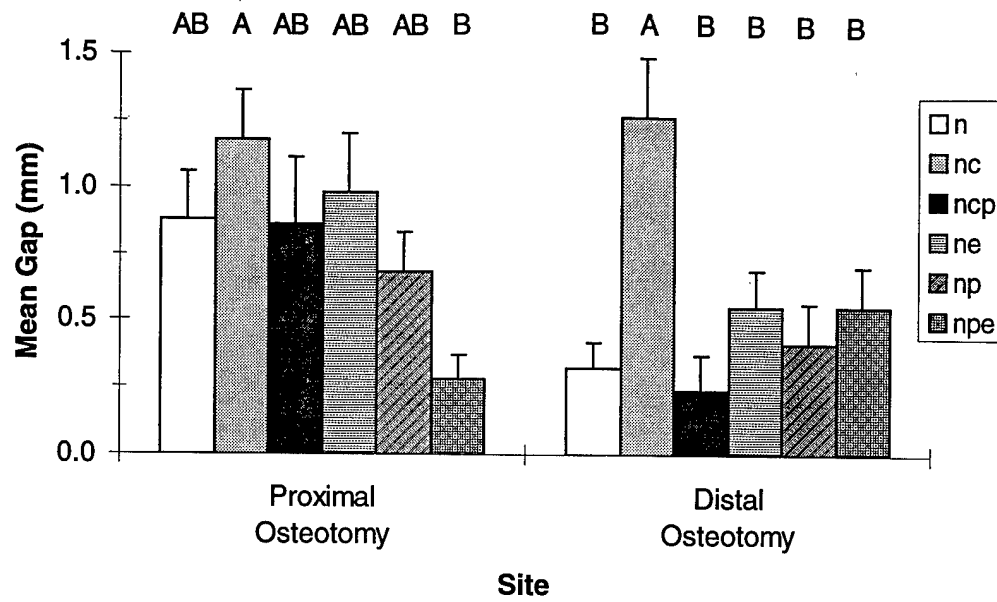


**Figure 11.** Mean gap ( $\pm$  SEM) of all quadrants determined from histologic sections of treatments at each osteotomy location. Letters above columns that differ indicate significance at that osteotomy ( $P < 0.05$ ).

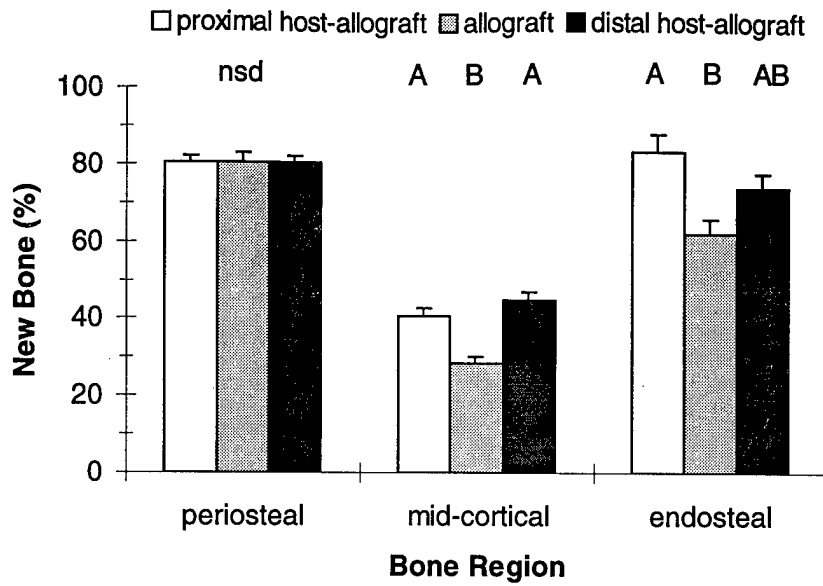


**Figure 12.** New bone formation (mean  $\pm$  SEM) determined from fluorescence of tetracycline labeled bone. New bone is expressed as the percent of fluorescent area relative to non-pore area. Letters above columns that differ indicate significance within the given region ( $P < 0.05$ ). nsd – no significant difference.